Non-diffusive Thermal Conduction in One-dimensional Materials

CHIH-WEI CHANG

CENTER FOR CONDENSED MATTER SCIENCES, NATIONAL TAIWAN UNIVERSITY

ABSTRACT

Non-diffusive thermal conduction was usually regarded as a phenomenon that exclusively occurred at very low temperatures or at the nanoscale range. In this article, I will present recent discoveries made by our group in Taiwan that demonstrate room temperature non-diffusive thermal conduction over micrometers in SiGe nanowires and over millimeters in carbon nanotubes. There are many interesting effects associated with non-diffusive thermal conduction that go beyond conventional knowledge of heat transfer. These discoveries could make wave-engineering of phonons possible and could pave the way for the development of new applications in phononics.

INTRODUCTION

Thermal conduction in solids was described by Joseph Fourier's classic work published in 1822, in which heat conduction was formulated as a diffusive process. Under steady state conditions, Fourier's law is expressed as

$$J_Q = -\kappa \nabla T \qquad (1)$$

where J_Q is heat flux, T is temperature, and κ is the thermal conductivity. Fourier's seminal work must have also inspired Georg Ohm and Adolf Fick, who at later times respectively formulated diffusive phenomena for electrical conduction (Ohm's law, 1827) and gas diffusion (Fick's law, 1855).

Following Fourier's law, thermal conductance (K) of a sample, after getting rid of its geometrical properties, can be directly related to κ by

$$K = \kappa \frac{A}{L} \qquad (2)$$

where A is the cross sectional area and L is the sample length. Now, because κ is always found to be independent of sample geometry in all macroscopic materials, κ is usually regarded as an intrinsic property of (bulk) materials. Thus, each bulk material has its own κ, which spans from $\kappa > 2000$W/m-K for a diamond to <0.1W/m-K for layered WSe$_2$ along the c-axis. Recently, it also has been found that boron arsenide (BAs) exhibits $\sim$1000W/m-K at room temperature.

Currently, we attribute heat transfer phenomena to be normal diffusion processes, in which particles undergo frequent collisions and make the spread of their distribution increase linearly with respect to time. Anomalous diffusion will occur if the linear relationship is broken down. Anomalous diffusion is believed to be correlated with non-diffusive thermal conduction, in which κ becomes dependent on the sample length L:

$$\kappa \propto L^\alpha \qquad (3)$$

That is, non-diffusive thermal conduction occurs when $\alpha > 0$. Non-diffusive thermal conduction can be further categorized into ballistic ($\alpha = 1$) and anomalous ($\alpha < 1$) thermal conduction that will be respectively discussed as follows.

BALLISTIC THERMAL CONDUCTION

According to our previous description of the diffusive process, heat conduction can be understood as energy-

carrying particles (i.e. phonons) undergoing frequent collisions so that the energy of hot phonons gradually transfers into the cold region. Between each collision process, the phonons can propagate without dissipation and the thermal conduction is said to be ballistic. So the characteristic length associated with the distance that phonons can travel without collisions is called the phonon mean free path (l). Following this definition, we can in principle determine the phonon mean free path of a sample by measuring its thermal resistance for various sample lengths (L), varying from $L < l$ to $L > l$, as shown in Fig. 1(a).

As shown in Fig. 1(b), when $L < l$, the sample is a ballistic thermal conductor, and the measured total thermal resistance ($1/K_{total}$) would only occur at the two boundaries between the sample and hot/cold heat baths. Length-independent thermal resistance occurs when $L < l$. When $L > l$, collision processes start to destroy the wave properties of phonons; one then has the ordinary result obeying Fourier's law, i.e. $1/K_{total}$ increases linearly with L, or equivalently, κ is length-independent, as shown in Fig. 1(c).
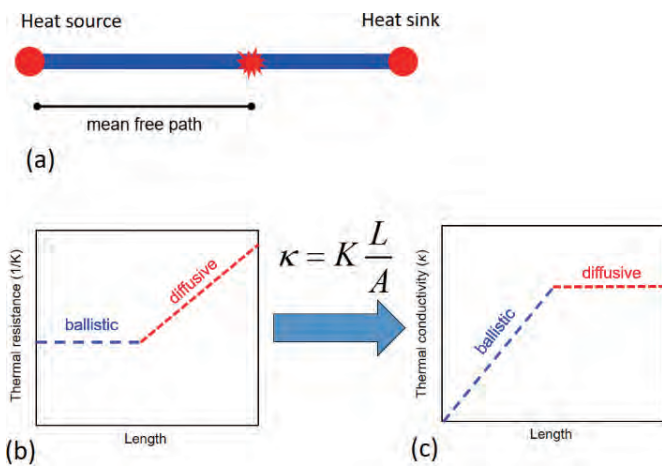
Fig. 1: (a) An illustration of a ballistic thermal conductor connected to a heat source and a heat sink. The phonon scattering event inside the sample destroys the wave properties of phonons and leads to a finite phonon mean free path. (b & c) The corresponding data when probing the length dependent thermal transport of (a). Both $1/K$ vs. L (b) and κ vs. L (c) relations are plotted here. Here, the contact thermal resistance is assumed to be zero in the diffusive regime.

When applying Eq. (2) to convert the measured K_{total} to κ_{total}, one sees that κ_{total} decreases when $L < l$ and saturates at a constant value when $L \gg l$, as shown in Fig. 1(c). For this reason, the observation that κ_{total} decreases with decreasing L is often regarded as a signal of ballistic thermal conduction.

However, there could be contact thermal resistance ($1/K_c$) in the probed system that plays an important yet subtle role in many experiments. After incorporating $1/K_c$, the experimentally measured total thermal resistance ($1/K_{total}$) can be expressed as:

$$\frac{1}{K_{total}} = \frac{1}{K_{sample}} + \frac{1}{K_c} \qquad (4)$$

where $1/K_{sample}$ is thermal resistance and we assume K_c is a constant. Now, if we probe a purely diffusive thermal conductor (i.e. $1/K_{sample} = aL$ ($a > 0$)) in the presence of $1/K_c > 0$, κ_{total} follows

$$\kappa_{total} \equiv \frac{K_{total}L}{A} = \frac{L/A}{aL + 1/K_c} \qquad (5),$$

which also leads to $\kappa_{total} \to 0$ as $L \to 0$. The behavior could be easily mistaken as the signal for ballistic thermal conduction! To illustrate the fallacy, we plot κ_{total} vs. L and $1/K_{total}$ vs. L in Fig. 2, with added noises to simulate the experimental data. If one merely focuses on the decrease of κ_{total}, the phonon mean free path l could be erroneously identified to be larger than 10, significantly deviating from the correct value ($l = 0$) [1].

To correctly identify the ballistic thermal conduction from the experimental data, it is recommended to plot the $1/K_{total}$ vs. L relation. The $1/K_{total}$ vs. L relation would allow us to separate the ballistic thermal conduction from the unwanted effect of contact thermal resistance by reading the offset at $L \to 0$, as shown in Fig. 2(b). The ballistic thermal conduction can be seen by observing the
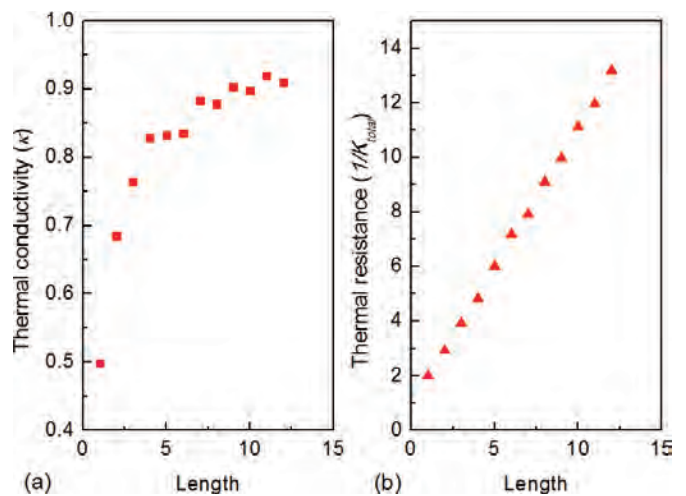
Fig. 2: Simulated (a) κ_{total} vs. L and (b) $1/K_{total}$ vs. L relations for $1/K_c = 3$. It can be seen that finite contact thermal resistance will create a fallacious ballistic thermal conduction effect in the κ_{total} vs. L relation even if the sample is a diffusive conductor [1].

Fig. 3: κ_{total} vs. L and $1/\kappa_{total}$ vs. L relations for (a & b) Si [2], (c & d) sapphire, Si, and $Si_{0.992}Ge_{0.008}$ [3], and (e & f) BAs, boron nitride (BN), and diamond [4,5], replotted from the respective papers. It can be seen that although all κ_{total} vs. L data suggest ballistic thermal conduction over several micrometers, $1/\kappa_{total}$ vs. L relations display no clear deviations to diffusive thermal conduction except for GaAs at 180K and BAs for $L<3\mu m$.

deviation from diffusive behavior, i.e. $1/K_{total}$ would be larger than what it should be when extrapolating from the data of large L's.

Unfortunately, not many researchers are aware of the possibility of contact thermal resistance in their systems and the importance of plotting thermal resistance vs. length to correctly determine the phonon mean free path. For example, Johnson et al. employed laser-induced transient thermal gratings to measure in-plane thermal diffusivity of Si membranes [2]. The deduced κ_{total} vs L is shown in Fig. 3(a). From Fig. 3(a), we see that the κ_{total} quickly decreases as L is shorter than 3μm, which led them to conclude that the phonon mean free path of Si is at the micron scale at room temperature. However, if we replot the data into (normalized) thermal resistance A/K_{total} vs. L, we simply see purely diffusive thermal conduction (i.e. $1/K_{total}$ is linearly proportional to L added with a finite $1/K_c$, as shown in Fig. 3(b).) It demonstrates that the presence of $1/K_c$ could easily mislead researchers to overestimate the phonon mean free paths. Similarly, Hu et al. employed time-domain thermoreflectance measurements to study thermal diffusivities of sapphire, Si, and $Si_{0.992}Ge_{0.008}$ and claimed to observe ballistic thermal conduction over micron-scales [3]. But when replotting the same data into $1/K_{total}$ vs. L, we could only observe diffusive thermal conduction, as shown in Fig. 3(c & d). Similar problems also exist in the recently-discovered BAs, in which we found that the length of ballistic thermal conduction is much shorter than claimed [4,5], as shown in Fig. 3(e & f).

We recognize these issues. So when determining phonon mean free path of SiGe nanowires, we will need to provide very solid and rigorous proof for ballistic thermal conduction. SiGe nanowires are a model alloy system in which the role of alloy scatterings of phonons in nanoscale dimensions can be thoroughly investigated. Interestingly, theoretical predictions on the phonon mean free path of SiGe vary five orders of magnitudes. The large discrepancies have motivated us to experimentally measure its phonon mean free path [6].

Our $Si_{1-x}Ge_x$ (x = 0.1 ~ 0.6) nanowires were grown by the chemical vapor deposition method. The nanowires were found to exhibit homogeneously-alloyed structures for x=0.1 and imperfect twin boundaries and compositional variations for x~0.6. Interestingly, the ballistic thermal conduction discussed later does not seem to be affected by these perturbations.
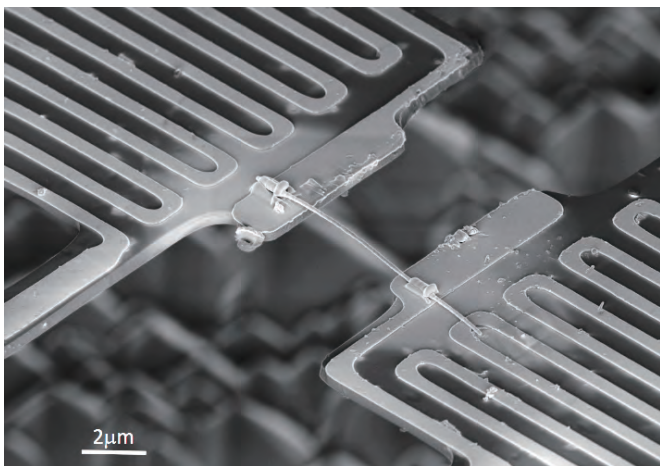
Fig. 4: SEM image of a thermal conductivity test fixture consisting of a suspended heater and sensor pads with a SiGe nanowire anchored on it [6].

To measure the thermal conduction of individual SiGe nanowires, we fabricated microscale thermal conductivity test fixtures consisting of suspended heaters and sensors, shown in Fig. 4 [6]. The thermal conductivity test fixture consisted of two suspended silicon nitride (SiN$_x$) membranes each supported by five 420μm-long and 2μm-wide SiN$_x$ beams. Nanowires with chosen lengths or diameters were picked up and placed on the test fixture by a sharpened tungsten tip operated by a piezodriven manipulator inside a scanning electron microscope (SEM). In-situ deposition of Pt/C composites was then carried out to rigidly bond the nanowire to the test fixture. To measure the total thermal conductance (K_{total}) of the system (i.e. including the nanowire and contact ther-

mal resistance), Joule heating was supplied to the heater and the temperature rises of the heater and sensor were measured. Under steady state, K_{total} can be obtained using the relation

$$K = \frac{P}{\Delta T_H - \Delta T_S}\left(\frac{\Delta T_S}{\Delta T_H + \Delta T_S}\right) \quad (6)$$

where P is the Joule heating power, ΔT_H and ΔT_S is the raised temperature on the heater and the sensor, respectively. Due to the linear relation of resistance with respect to temperature of the Pt film resistors, the temperature variations of the heater and the sensor can be directly obtained by measuring their resistance. The thermal conductivity κ_{total} was evaluated by incorporating the length and the cross sectional area (A) of the nanowire determined by SEM. As emphasized earlier, κ_{total} could include contact thermal resistance of the system. The measurements were carried out at pressure $<10^{-5}$ mbar to eliminate unwanted heat conduction or convection.
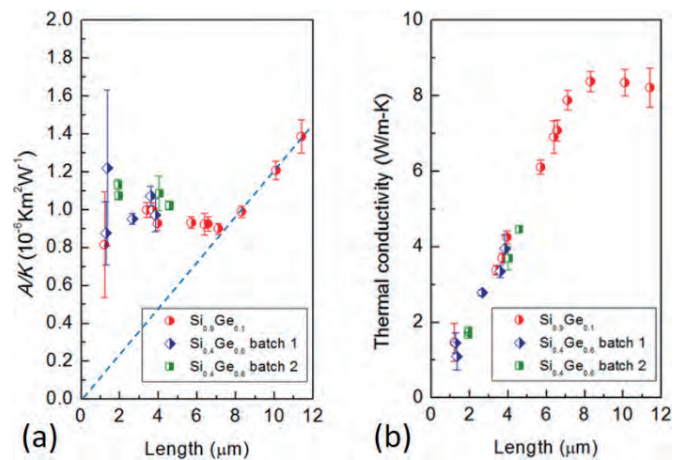
Fig. 5: (a) A/K_{total} vs. L and (b) κ_{total} vs. L relations for homogeneously-alloyed SiGe nanowires. Both κ_{total} vs. L and A/K_{total} vs. L relations deviate from the diffusive behavior for $L < 8$μm, indicating ballistic thermal conduction. The blue dashed line is a fitted line extrapolating from data of $L > 8$μm [6].

We have systematically measured the length dependent thermal transport for more than twenty SiGe nanowires of different diameters, structures, and alloy concentrations. Due to the variations of the cross sectional areas between different samples, we plotted the normalized thermal resistance (A/K_{total}) vs. L relation in Fig. 5(a). A/K_{total} decreases linearly with L for $L > 8$μm, indicating the expected diffusive transport behavior. Interestingly, A/K_{total} vs. L changes the slope at $L = 8$μm and it significantly deviates from the diffusive behavior for $L < 8$μm.

Because of the strong deviation to the diffusive behavior and the agreement with the determination of phonon mean free path described earlier, we attribute the effect for $L < 8\mu m$ to be ballistic thermal conduction at room temperature, which was not observed in other materials of comparable length scales at room temperature. Moreover, extrapolating the diffusive behavior ($L > 8\mu m$) to $L \rightarrow 0$ suggests that the (classical) contact thermal resistance is nearly zero. After plotting the data into κ_{total} vs L in Fig. 5(b), we now see clearly that the κ_{total} decreases with decreasing L for $L < 8\mu m$ cannot be attributed to effects of finite contact thermal resistance. Instead, the behavior is entirely due to ballistic thermal conduction.

Extrapolating the ballistic thermal resistance ($L < 8\mu m$) to $L \rightarrow 0$ leads to finite contact thermal resistance, which also reveals interesting effects. Surprisingly, we find that small deviations to the dashed line in Fig. 5(a) are observed even when the investigated SiGe nanowires have very different contact geometries to the heat baths. Indeed, Fig. 5(a) shows that contact thermal resistance is inversely proportional to cross sectional area of the nanowire rather than the real contact area between the nanowire and the heater/sensor pads. The counter-intuitive result is in fact due to the occurrence of ballistic thermal conduction that constrains the phonons to enter into limited heat conduction channels of a nanowire. We would call this quantum contact thermal resistance as it originates from mode mismatches between phonons in the heat bath and the nanowire. Because the effect originates from the wave nature of phonons, we regard this interesting observation as the second evidence for ballistic thermal conduction of SiGe nanowires [6].

Ballistic thermal conduction also displays more interesting phenomena when connecting two nanowires in series. Connecting two diffusive or two ballistic thermal conductors in series is known to yield distinct results on the total thermal conductance (K_{total}):

$$K_{total} \leq \begin{cases} (K_1, K_2)_{\min} & \text{for ballistic conductors} \\ K_1 K_2 / (K_1 + K_2) & \text{for diffusive conductors} \end{cases} \quad (7)$$

where the inequality holds when the classical contact thermal resistance at the junction is nonzero. $(K_1, K_2)_{\min}$ denotes the minimum value of the set (K_1, K_2). Note that Eq. (7) has taken into account the classical contact resistance so the K_{total} should never exceed $K_1 K_2 / (K_1 + K_2)$ for two diffusive conductors connected in series. Because of the characteristically different sum rules, any violations

of the inequality of the diffusive thermal conductors in Eq. (7) will be evidence of ballistic thermal conduction. Thus, experimentally testing the inequalities shown in Eq. (7) is an independent method for checking the ballistic thermal conduction found in Fig. 5.
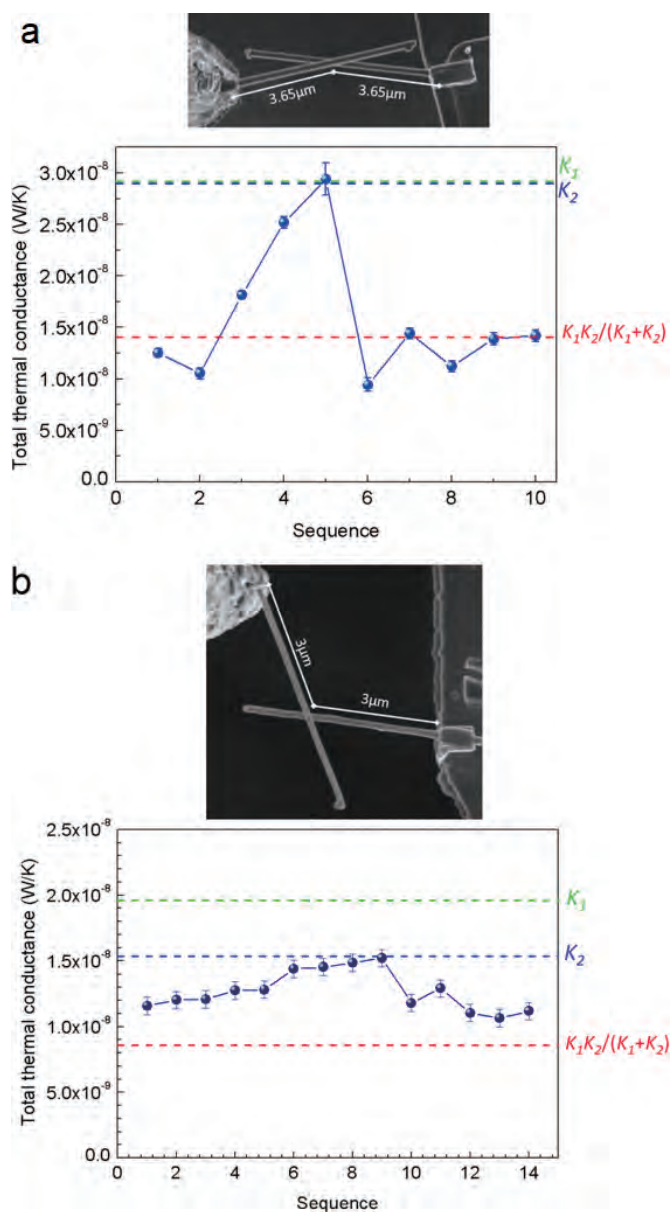
Fig. 6: (a) (Upper) A representative SEM image when we rubbed, pressed, or rotated the two mechanically-touched SiGe nanowires against each other using a manipulator. The process allows us to survey many possible thermal contact configurations between two SiGe nanowires. (Lower) Measured K_{total} during the sequence. (b) An SEM image of two SiGe nanowires of dissimilar diameters mechanically connected and repeated a similar sequence described in (a). (Lower) Measured K_{total} during the sequence. The green, blue, and red dashed lines denote the values of K_1, K_2, and $K_1K_2/(K_1+K_2)$, respectively. The blue/red dashed line also denotes the maximum K_{total} allowed from Eq. (7) for ballistic/diffusive thermal conductors [6].

To carry out the experiment, we employed a manipulator to connect two nanowires in series [6]. Figure 6(a) displays the measured K_{total} of two SiGe nanowires of similar diameters connected in series ($d_1 \sim d_2 = 183$nm). In order to minimize the effect of contact thermal resistance at the junction, we sequentially rubbed, rotated, and pressed the two nanowires against each other. At sequence 3, 4, and 5, the data clearly exceeded the limit predicted by diffusive conductors. It is because the total length ($L_1 + L_2 = 7.3$μm < 8μm) is within the ballistic transport regime; the whole system still behaves like a ballistic thermal conductor (with added phonon scatterings at the junction). Remarkably, perfect ballistic phonon transmission (i.e. $K_{total} = (K_1, K_2)_{min}$) is observed at sequence #5, indicating that the phonon scatterings at the junction can be reduced to zero.

Figure 6(b) displays the measured K_{total} of another two SiGe nanowires of dissimilar diameters ($d_1 = 158$nm, $d_2 = 140$nm) connected in series. Again, all the data shown in Fig. 6(b) disobeyed the inequality of Eq. (7) for diffusive conductors. Instead, the K_{total}'s followed the inequality for ballistic thermal conductors and the largest values (sequence #8, 9 in Fig. 6(b)) were equal to $(K_1, K_2)_{min}$. Thus, these results provided a third piece of evidence regarding ballistic thermal conduction of SiGe nanowires at room temperature [6].

ANOMALOUS THERMAL CONDUCTION

Thermal conduction in one-dimensional (1D) systems has been a controversial subject since the 1940s; it can be summarized by quoting Peierls [7]: "It seems there is no problem in modern physics for which there are on record as many false starts, and as many theories which overlook some essential feature, as in the problem of the thermal conductivity of (electrically) non-conducting crystals." In 1D systems, κ is no longer an intrinsic properties of materials, and it could increase with increasing sample length, i.e. $\kappa \sim L^{\alpha}$ with an anomalous ($\alpha < 1$) exponent.

Despite intensive work on the problems of 1D thermal conduction, theoretical disputes on many anomalous effects have not been completely settled. For example, while the power law divergence of κ's in 1D models have been known to be insensitive to disorders, it is not clear whether there exists a universal α for all 1D systems [8]. Even though the renormalization group analyses have suggested a universal $\alpha = 1/3$ [9], various numerical results have indicated otherwise [10,11]. Moreover,

mode-coupling theory and molecular dynamics simulations have suggested a wide range of α's depending on the temperatures, diameters, and chiralities of a quasi-1D system like a single-wall carbon nanotube (SWCNT) [12,13]. In fact, the only consensus seems to be that breaking momentum conservation would lead to $\alpha = 0$ in 1D systems [14].

The above theoretical works are all based on toy models. For calculations on realistic materials, solving the Boltzmann transport equation suggests that the κ will saturate at a constant value for a defect-free, sufficient long (10μm $\sim$ 1mm) SWCNT [15,16]. However, the result contradicts with many studies based on molecular dynamics (MD) simulations [12,17-19]. Even so, it must be pointed out that many MD simulations are inconsistent with each other.

A realistic material will always have defects or vacancies. Calculations based on the Boltzmann transport equation also suggest that these disorders in a SWCNT can remove the contributions of low frequency phonons and facilitate the saturation of κ at much shorter lengths [15]. However, it is not clear why a quasi-1D system like a SWCNT could show normal heat conduction behavior when both 1D and 2D systems are known to be non-Fourier thermal conductors. All of these fundamental disagreements between different theories urgently await experimental input.
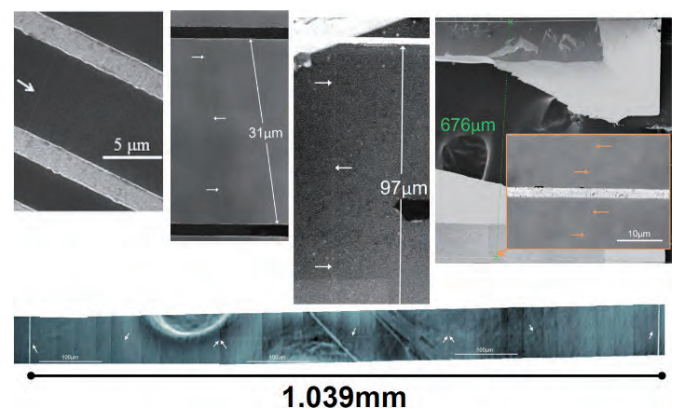
Fig. 7: Representative SEM images of individual CNTs suspended on the test fixture. The suspended length varies from 4μm to 1039μm [20].

To rigorously study the fundamental heat transfer phenomena, we have considerably improved the material syntheses and the measurement sensitivities over previous setups [20]. Ultralong SWCNTs with lengths exceeding 2cm were grown using chemical vapor deposition
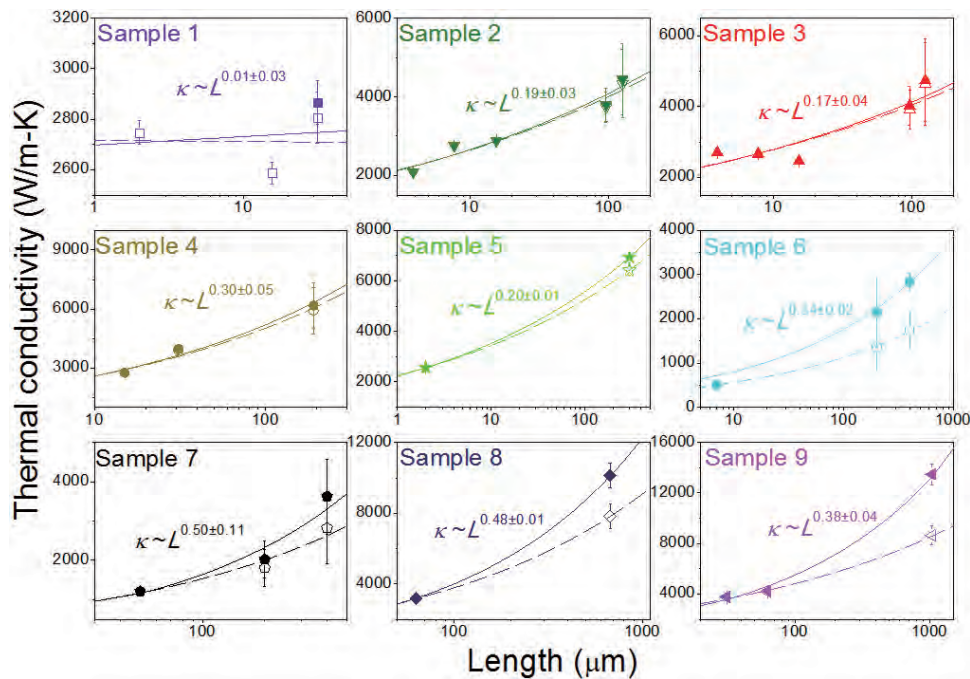
Fig. 8: Measured κ_{total}'s (open symbols) and corrected κ's (solid symbols, after incorporating radiation heat loss from the surface of SWCNTs) are shown for each sample. For the longest SWCNT investigation ($L = 1.039$mm), the measured κ_{total} and the corrected κ reached 8640 W/m-K and 13300 W/m-K, respectively. The fits (by parametrizing $\kappa \sim L^\alpha$) to the corrected κ's and measured κ_{total}'s are shown by solid curves and dashed curves, respectively [20].

methods and anchored on our tailored thermal conductivity test fixtures consisting of suspended SiN$_x$ beams. As shown in Fig. 7, the L's of the investigated SWCNTs span from 2μm to 1.039μm. Note that the latter scale is much longer than the theoretical phonon mean free path of a SWCNT. Therefore, any deviations from diffusive thermal transport observed in our experimental data should not be confused with conventional ballistic thermal conduction.

Figure 8 shows the κ_{total} vs L of the investigated samples, while the κ_{total}'s of sample 2 to sample 9 display unambiguous divergent behavior with increasing L. No divergence of κ_{total} is observed in sample 1, possibly due to its relatively short L (< 30 μm). For the longest SWCNT ($L = 1.039$ mm), $\kappa_{total} = 8638 \pm 734$ W/m-K has been measured (assuming $d = 2$ nm), which is nearly three times larger than the κ of a diamond at room temperature.

Because of the heat loss by radiation from the surface of the ultralong SWCNTs, the power received by the sensor was and is always smaller than that transmitted from the heater. Thus, the measured κ_{total}'s simply set the lower bound for the actual values. In fact, after correcting the radiation loss, we estimated the intrinsic κ would be

6900 W/m-K for sample 5 ($L > 300$ μm), 10050 W/m-K for sample 8 ($L > 670$ μm), and 13300 W/m-K for sample 9 ($L > 1$ mm).

Furthermore, the effect of contact thermal resistance has been eliminated because of the experimentally investigated L's span of 3 orders of magnitude; yet, the contact area has remained the same. Therefore, we concluded that the experimentally observed divergent behavior of κ and the ultrahigh κ originates from the intrinsic properties of the ultralong SWCNTs, but not from artifacts of thermal radiation or contact thermal resistance [20]. The comment raised by Li et al. [21] incorrectly applies the analyses of their setups into ours and thus the comment is wrong from the beginning [22]. Besides, our controlled experiment on an SiN$_x$ beam [20] and an independent experiment based on measuring κ_{total} vs. L of SiO$_2$ nanowires also confirm the correctness of our analyses [23].

On the other hand, Liu et al.'s experiment suggests a convergent thermal conductivity of SWCNTs at length (L) ~10μm [24], which seems to contradict with our results. But any experts who have had experience on employing Raman scattering as thermometers know it always has >10% uncertainty in the temperature measurement [10,21,22], and, additionally, has complex po-

sition dependent variations [10,22], these would render Liu et al.'s data inconclusive for $L > 5\mu m$.

Based on diffusive thermal transport, high thermal conductivity is always achieved in crystalline solids exhibiting strong chemical bonds and is independent of sample geometries. Since it is unlikely to synthesize new materials stronger than covalently-bonded carbon materials, the room temperature $\kappa \sim 3000$ W/m-K found in diamond, graphene, and SWCNTs is generally considered as an insurmountable limit for all materials. Here we report that the observation of non-diffusive heat conduction phenomenon in ultralong SWCNTs whose κ increases with lengths without signs of saturation, reached an unprecedented high value ~ 8640 W/m-K at room temperature for millimeter-long SWCNTs. Remarkably, the κ's of the investigated SWCNTs display power-law divergences even with the presence of isotopic disorders, defects, impurities, or surface absorbates. Thus, we demonstrate that the anomalous thermal conduction in real materials can persist over much longer distances than previously thought.

CONCLUSION

At room temperature, phonons have characteristic frequencies in the terahertz range. However, our current technologies lack the proper tools to characterize phonon properties in this frequency domain. This lack of knowledge and the dearth of useful tools to understand phonons has often made people call high frequency phonons "waste heat". Indeed, current heat management methods, based on diffusive transport, are akin to electronics based on Ohm's law before knowing Maxwell's equations. Room temperature non-diffusive thermal conduction, including micrometer-long ballistic thermal conduction and millimeter-long anomalous thermal transport, respectively found in SiGe nanowires and CNTs, could be the first step toward making use of the wave properties of phonons. We hope that more researchers will pay attention to this emergent field and will join us in exploring new domains for phononic applications in the future.

References

[1] B. W. Huang, T. K. Hsiao, K. H. Lin, D. W. Chiou & C. W. Chang. AIP Advances 5, 053202 (2015).
[2] J. A. Johnson et al. Phys. Rev. Lett. 110, 025901 (2013).
[3] Y. J. Hu, L. P. Zeng, A. J. Minnich, M. S. Dresselhaus & G. Chen. Nature Nanotechnology 10, 701 (2015).
[4] J. S. Kang, M. Li, H. A. Wu, H. Nguyen & Y. J. Hu. Science 361, 575 (2018).
[5] S. Li et al. Science 361, 579 (2018).
[6] T. K. Hsiao et al. Nature Nanotechnology 8, 534 (2013).
[7] R. E. Peierls. Theoretical Physics in Twentieth Theory. (Interscience, 1960).
[8] A. Dhar & K. Saito. Phys. Rev. E 78, 061136 (2008).
[9] O. Narayan & S. Ramaswamy. Phys. Rev. Lett. 89, 200601 (2002).
[10] P. L. Garrido, P. I. Hurtado & B. Nadrowski. Phys. Rev. Lett. 86, 5486 (2001).
[11] P. I. Hurtado. Phys. Rev. Lett. 96, 010601 (2006).
[12] G. Zhang & B. W. Li. J. Chem. Phys. 123, 114714 (2005).
[13] J. S. Wang & B. W. Li. Phys. Rev. Lett. 92, 074302 (2004).
[14] T. Prosen & D. K. Campbell. Phys. Rev. Lett. 84, 2857 (2000).
[15] N. Mingo & D. A. Broido. Nano Lett. 5, 1221 (2005).
[16] L. Lindsay, D. A. Broido & N. Mingo. Phys. Rev. B 80, 125407 (2009).
[17] S. Maruyama. Physica B 323, 193 (2002).
[18] S. Maruyama. Microscale Thermophys. Eng. 7, 41 (2003).
[19] K. Saaskilahti, J. Oksanen, S. Volz & J. Tulkki. Physical Review B 91, 115426 (2015).
[20] V. Lee, C. H. Wu, Z. X. Lou, W. L. Lee & C. W. Chang. Phys. Rev. Lett. 118, 135901 (2017).
[21] Q. Y. Li, K. Takahashi & X. Zhang. Phys. Rev. Lett. 119, 179601 (2017).
[22] V. Lee, C. H. Wu, Z. X. Lou, W. L. Lee & C. W. Chang. arXiv:1806.11315 (2018).
[23] Renkun Chen, private communication
[24] J. H. Liu, T. Y. Li, Y. D. Hu & X. Zhang. Nanoscale 9, 1496 (2017).
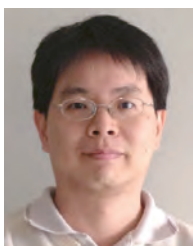
Chih-Wei Chang is currently an associate research fellow of the Center for Condensed Matter Sciences at National Taiwan University. He received his PhD (2006) in physics from the University of California at Berkeley, focusing on experimental thermal transport measurements of nanomaterials. He was a postdoctoral researcher at the Nanoscale Science and Engineering Center at UC Berkeley, studying topics of plasmonics and metamaterials. After returning to Taiwan in 2009, his research interests have continued to cover various topics on nanoscale phononics and photonics.